RESEARCH ARTICLE | NOVEMBER 11 2024

Non-destructive characterization of individual particle bunches by a resistive-cooling measurement in a Penning trap

Markus Kiffer ; Stefan Ringleb ; Thomas Stöhlker ; Manuel Vogel

J. Appl. Phys. 136, 184901 (2024)
https://doi.org/10.1063/5.0228725

Journal of Applied Physics ARTICLE pubs.aip.org/aip/jap

Non-destructive characterization of individual particle bunches by a resistive-cooling measurement in a Penning trap

Cite as: J. Appl. Phys. **136**, 184901 (2024); doi: 10.1063/5.0228725
Submitted: 15 July 2024 · Accepted: 28 October 2024 ·
Published Online: 11 November 2024

Markus Kiffer,[1,a] Stefan Ringleb,[1,b] Thomas Stöhlker,[1,2,3] and Manuel Vogel[3]

AFFILIATIONS

[1]Friedrich Schiller-Universität Jena, 07743 Jena, Germany
[2]Helmholtz-Institut Jena, 07743 Jena, Germany
[3]GSI Helmholtzzentrum für Schwerionenforschung, 64291 Darmstadt, Germany

[a]**Author to whom correspondence should be addressed:** markus.kiffer@uni-jena.de
[b]**Electronic mail:** stefan.ringleb@uni-jena.de

ABSTRACT

We have developed and operated an electronic system for the non-destructive detection and cooling of charged-particle bunches that are captured and confined in a Penning trap, together with methods for the evaluation of corresponding measurements that allow for a detailed characterization of each individual particle bunch. Once calibrated, from a single measurement of the particles' induced electronic signal as a function of time directly upon capture, the setup and method allow for a fast determination of the initial and final absolute particle energies, of the cooling rate, and of the absolute number of particles in the bunch. We demonstrate this with highly charged ions (Ne^{8+}) that are injected into the Penning trap of the HILITE experiment.

I. INTRODUCTION

The method of resistive cooling of charged particles in a Penning trap is well-established and well-understood particularly for single particles[1–3] but also for ensembles of particles.[4,5] It is based on image currents that the particle motions induce in the conducting trap electrodes.[6–8] When these currents are damped by resistive elements, the motion of the particles is damped in turn.

Most often, resistive cooling is applied to the axial particle oscillation in the trap by means of a tuned resonant circuit that is either placed across a pair of electrodes or that connects one electrode to the ground. The real part of the circuit's impedance dissipates energy from the axial motion into the cold bath in which the circuit is embedded.[9–11] This reduces the axial particle energy and, hence, the amplitude of the oscillation, until the temperature associated with that energy comes into equilibrium with the cold bath, often at liquid-helium temperature.[11]

The benefit of such cooling is a significant reduction in the particles' axial velocity and spread, which facilitates well-defined confinement close to the trap center and the conditions required for a number of spectroscopic precision measurements across a wide range of frequency domains.[9]

For resistive cooling of large particle ensembles, it has been shown that only the center-of-mass motion is directly cooled by the interaction with the circuit, while all other motions are indirectly cooled only to the extent of their energy transfer into the center-of-mass motion.[9] For the axial motion, one expects and observes a fast cooling of the center-of-mass motion with an exponential cooling rate that is proportional to the number of particles, and a de-phasing of the axial motions due to residual imperfections of the initial ensemble and the trapping fields.[10] In previous measurements,[10] more than 99.99% of the initial center-of-mass axial particle energy was cooled away resistively within about 50 ms. We have also previously shown that a comparatively simple model for the energy flow within the particle–circuit system can account for the observed effects during resistive cooling.[10]

One can create a particularly clear-cut situation when particle capture[12] into the trap is done along the central trap axis (thus

avoiding significant initial magnetron motion) and when the particles form a well-defined bunch that occupies a small volume in phase space, i.e., has both a small spatial and velocity spread. This translates into a narrow distribution of the axial frequencies and phases of motion of the stored particles. Then, the initial axial kinetic energy is concentrated in the axial center-of-mass motion of the incoming particle bunch. This axial center-of-mass energy can be cooled away efficiently before the bunch has a chance to de-phase into uncorrelated motions that are far less efficiently cooled.[10]

When the cooling circuit is chosen to connect a pair of electrodes with mirror symmetry with respect to the trap center, rather than connecting one electrode to the ground, it becomes insensitive to electronic noise due to fast switching and pulsing of electrodes as required for the dynamic capture of externally produced particles.[12]

In the following, we show how this can be used to determine the initial axial particle energy directly upon trapping, the final axial particle energy, the rate of cooling, and the number of particles within the bunch. Apart from a characterization of the cooling process, this may be used, e.g., for an optimization of the injection and capture process and to determine the number of stored ions which is of high interest, i.e., for the measurement of absolute cross sections in laser-ionization experiments.[13]

The measurements have been performed with Ne^{8+} ions from an external source that are injected into the Penning trap of the HILITE experiment.[13] They complement earlier demonstrations of non-destructive characterization of particle bunches in a beamline,[14,15] in the sense that the present methods find application directly inside the trap and at much lower kinetic energies and can, hence, be used to infer the properties of the confined particles directly before a subsequent measurement.

II. ION MOTION AND COOLING IN A PENNING TRAP

We consider a cylindrical Penning trap[16,17] located in the center of a homogeneous magnetic field B_0 that is produced by a superconducting magnet. The central trap axis and the magnetic field axis are identical and defined to be the z-axis (see also Fig. 1). Voltages applied to the trap electrodes form a quadrupolar electrostatic potential with the well $V \propto z^2$ along z. Any individual ion in this field configuration performs a motion that is comprised of an axial oscillation about the trap center at $z = 0$ and a radial motion that is a cyclotron orbit around the magnetic field, perturbed by a drift motion in the crossed electric and magnetic fields (magnetron motion).[9]

These motions have frequencies ω_z (axial frequency), ω_+ (reduced cyclotron frequency), and ω_- (magnetron frequency), respectively, with $\omega_+ \gg \omega_z \gg \omega_-$. For any given ion species and trap, the values of these frequencies are uniquely determined by the values of the confining fields.[2,9] For negligible field imperfections ("ideal trap"), the energies (amplitudes) of the three motions are independent of each other and have no effect on any of the motional frequencies.[2] The axial frequency is given by

$$\omega_z = \sqrt{\frac{qV}{md^2}}, \tag{1}$$

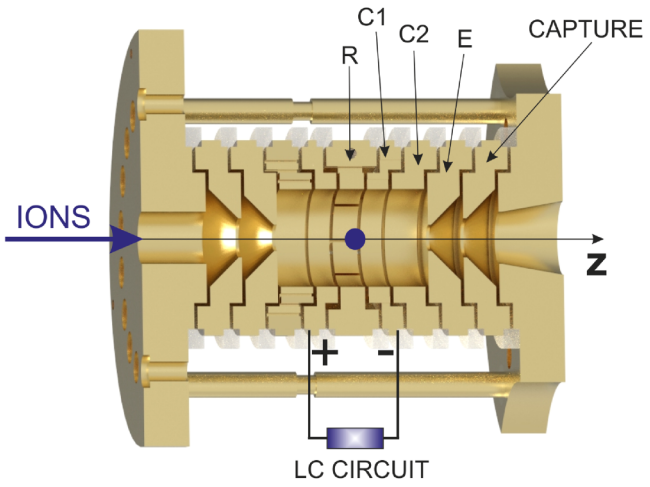

FIG. 1. Sectional view of the Penning trap with the ring (R), two pairs of correction electrodes (C1 and C2), endcaps (E), and additional capture electrodes. Ion bunch injection from the left is indicated, as well as a confined ion bunch in the trap center, and the electronic circuit that connects the two inner correction electrodes C1. The trap has mirror symmetry, so only one half is labeled.

where V is the depth of the electrostatic potential well and d is a measure of the trap size.[16] At present, the axial frequency is of the order of MHz.

Since we are interested in the behavior of many identical particles that initially form a bunch, we adopt the center-of-mass picture, i.e., we describe the bunch by its axial center-of-mass motion and by the axial individual-ion motions relative to it. For the present conditions, a significant amount of energy is initially concentrated in the center-of-mass motion,[10] i.e., before and directly upon capture, the ions form a well-defined bunch that occupies a small phase space. During confinement, the ions move with a fixed phase initially and begin to de-phase due to their initial axial energy spread and due to residual imperfections of the confining fields, which make the axial oscillation frequencies slightly dependent on the kinetic energies of the individual ions.[2,5] This leads to a re-shuffling of axial energy between the center-of-mass and individual motions at a rate γ_{ax} that is given by the width of the axial frequency distribution within the ion bunch at any time.[1]

First looking at the axial motion of a single ion during resistive cooling, the ion kinetic energy decays like

$$E(t) = E(0)\exp(-\gamma t), \tag{2}$$

where $E(0)$ is the initial axial energy of the ion. It is assumed to be much larger than the energy that corresponds to the temperature of the cold bath of the electronic cooling circuit, i.e., we have $E(0) \gg k_B T$. At present, this is true since $E(0)$ is of the order of eV, while $k_B T$ is below meV at liquid-helium temperature.

For a single ion, the exponential cooling rate in Eq. (2) is given by[5]

$$\gamma \equiv \gamma_1 = \frac{q^2 R}{mD^2}, \tag{3}$$

where R is the real part of the circuit's impedance Z at the axial oscillation frequency ω_z and D measures the effective distance of the electrodes used for cooling from the trap center.[9] For the present conditions, the value of γ_1 is about 0.005 s^{-1}.

It can be shown[3,9] that the resistive cooling of the total energy of an ensemble of identical ions with **random phases** of motion occurs at the same rate as the single-ion cooling given by Eq. (3), irrespective of the number of ions N.

However, when looking at the center of mass of an ion bunch, the situation is equivalent to an ion ensemble that moves **in phase** ("coherently"), and we can regard it as a single ion with mass Nm and charge Nq. This leads to an exponential cooling rate of[9]

$$\gamma \equiv \gamma_N = \frac{(Nq)^2 R}{(Nm)D^2} = N\frac{q^2 R}{mD^2} = N\gamma_1, \tag{4}$$

which is exactly N times faster than the single-ion cooling rate from Eq. (3).

The actual rate of cooling that is observed in an experiment depends on the initial conditions and their evolution during cooling, in particular on the distribution of axial oscillation frequencies and of the phases of axial motion. This means that in general, we expect the observed rate of cooling to change over time. We will discuss this in detail in the framework of the cooling model presented below.

III. SETUP AND PROCEDURES

The current measurements have been performed with the setup of the HILITE experiment[13] located at the Helmholtz Institute Jena, Germany.

A. Overview

The setup and methods have been described in detail previously.[13–15] In short, bunches of highly charged ions are produced in a commercial electron-beam ion trap (EBIT)[21] and selected (with respect to their charge-to-mass ratio) by a Wien filter.[22] The pure ion bunches (presently Ne^{8+}) are then guided by a low-energy electrostatic beamline to the Penning trap of the experiment. This is located in the center of a horizontal-bore superconducting magnet that can produce static fields up to $B_0 = 6$ T. A system of position-sensitive non-destructive ion detectors[15] and ion optics[23] outside of the magnet is used to inject the ion bunches along the central trap axis, thus avoiding significant magnetron motion upon capture. Typically, 95% of the ions are injected and confined within about 100 μm from the central axis.[10] A pulsed drift tube[24] is used to decelerate the ion bunches from an initial energy of around 2 keV to roughly 150 eV per charge and ion. The final deceleration is achieved by a floating ground potential of the whole trap[25] such that each ion enters with an axial kinetic energy of about 20–30 eV per charge. This value has been established by lowering the trap potential V and observation of the ion loss. The ions are dynamically captured into the trap by fast switching of the trap potential on the entrance side.[12] Then, the individual trap voltages are chosen such that the trap forms a harmonic axial potential $V \propto z^2$ directly upon ion capture. The measurements to be discussed commence immediately upon dynamic capture.

B. Trap and electronics

The trap is a cylindrical Penning trap[16,17] that consists of a central ring electrode, two pairs of correction electrodes, one pair of endcaps, and additionally one pair of electrodes for dynamic capture.[12] It has the common axial symmetry and mirror symmetry with respect to the trap center, which is located in the center of the ring electrode. The endcap electrodes have a separation of 22.4 mm, and the inner diameter of the trap is 15 mm. The outer electrodes have a central hole with a diameter of 4 mm to allow for loading the trap with the externally produced ions (entry side, left) and for the axial ejection of the trap content onto an external detector with imaging capabilities (exit side, right).

The electronic circuit for detection and cooling is a normal-conducting resonant LC circuit made of high-purity copper wire wound around a toroidal polytetrafluorethylene (PTFE) core. It connects the two inner correction electrodes of the trap, rather than connecting one electrode to ground. The details and benefits of this design have been described previously.[17] The LC circuit has a resonance frequency of $f_0 = 1.38$ MHz and a quality factor of $Q = 11.5$.

C. Detection: Induced current

For a single charged particle, the induced current in the axial direction is given by[6,7,9]

$$I_\pm = -q\dot{z}\Gamma_\pm(z), \tag{5}$$

where q is the particle charge, $\dot{z}$ is its axial velocity, and the coupling strengths $\Gamma_\pm$ reflect the geometry and position of the + and − pick-up electrodes (C1 correction electrodes) with respect to the trap center (see also Fig. 1). Since both ends of the resonator are connected to a pick-up electrode, the total driving current is the difference of these currents,

$$I_{\mathrm{ind}} = I_+ - I_- = -q\Gamma(z)\dot{z}. \tag{6}$$

The resulting function $\Gamma(z)$ is shown in Fig. 2. Typically, the inverse quantity $D = \Gamma^{-1}$ is used to describe resistive cooling [see Eqs. (3) and (4)], but, here Γ is the more convenient quantity. The value of $\Gamma = 83.5\ \mathrm{m}^{-1}$ in the trap center corresponds to $D = 12$ mm.

In many experiments with confined and cooled particles, it is sufficient to consider the value of $\Gamma(z)$ at the trap center $z = 0$, because motional amplitudes are negligible with respect to the size of the electrode arrangement. Presently, however, this is not the case, since for dynamically captured ions from an external source, the particles may probe a considerable part of the trapping region initially. In this situation, it is possible to describe the coupling constant by a value $\hat{\Gamma}(a)$, which depends on the motional amplitude a in the z-direction. For a harmonic oscillation at frequency ω_z, the induced current has a period of $2\pi/\omega_z$. Hence, it can be

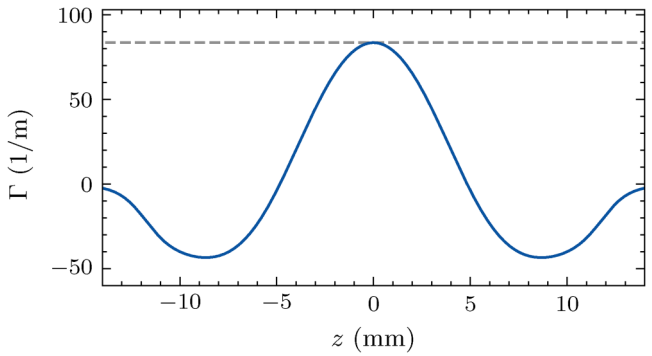

FIG. 2. Coupling constant Γ as a function of axial distance z from the trap center. The dashed value marks $\Gamma = 83.5\,\mathrm{m}^{-1}$ for $z = 0$, which corresponds to $D = 12$ mm.

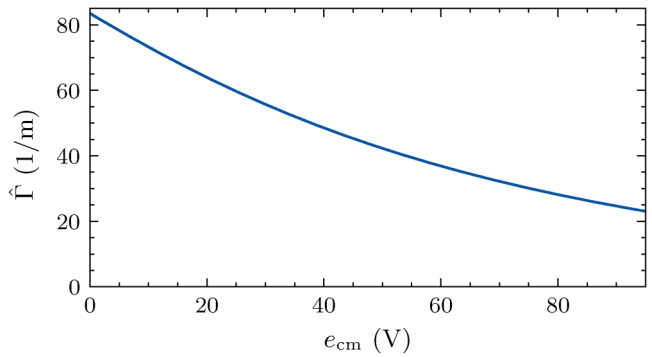

FIG. 3. Averaged result for $\hat{\Gamma}$ as a function of the center-of-mass energy e_{cm} according to Eq. (8).

expressed as a Fourier series by an expression of the kind

$$I_{\mathrm{ind}}(t) = -qa\omega_z \left[\sum_{k=1}^{\infty} A_k \cos(k\omega_z t) + B_k \sin(k\omega_z t) \right]. \tag{7}$$

From the series, only terms with frequency ω_z contribute to the measurement and the cooling process, as their multiples are far off resonance. For a harmonic motion $z \propto \sin(\omega_z t)$, the Fourier coefficients can be calculated by Eq. (6). Here, only the A_1 and B_1 terms contribute at frequency ω_z, and a calculation shows that $B_1 = 0$. Hence, the current is given by the A_1 term, which results in

$$I_{\mathrm{ind}}(t) = -q\hat{\Gamma}(a)\dot{z}, \quad \hat{\Gamma}(a) = \frac{2}{\pi}\int_{-1}^{1} \Gamma(as)\sqrt{1-s^2}\,\mathrm{d}s. \tag{8}$$

For a large ensemble of trapped particles in the center-of-mass picture, the total induced current is given by the approximation,

$$I_{\mathrm{ind}} = -Nq\hat{\Gamma}(a_{\mathrm{cm}})\dot{z}_{\mathrm{cm}}, \tag{9}$$

where a_{cm} is the center-of-mass amplitude and $\dot{z}_{\mathrm{cm}}$ is the center-of-mass velocity. This approach neglects possible non-linear currents induced by large-amplitude axial motions relative to the center of mass. For the present large ion ensembles with $N \gg 1$, such additional currents are expected to be insignificant compared to the induced current of the center-of-mass mode during initial cooling.[18] The resulting averaged value for $\hat{\Gamma}$ is shown in Fig. 3 as a function of center-of-mass energy per charge and particle e_{cm} by the identity,

$$a_{\mathrm{cm}} = \sqrt{\frac{2qe_{\mathrm{cm}}}{m\omega_z^2}}. \tag{10}$$

The results indicate that the value of $\hat{\Gamma}$ is smaller for larger oscillation amplitudes, which consequently reduces both the cooling efficiency and the signal strength. For $e_{\mathrm{cm}} = 0$, this reproduces the earlier result of $\Gamma = 83.5\,\mathrm{m}^{-1}$ in the trap center ($z = 0$), which corresponds to $D = 12$ mm. For larger energies (amplitudes), the coupling strength (signal pick-up) decreases significantly, which has to be taken into account in the further considerations.

One consequence is that the center-of-mass cooling rate γ_N from Eq. (4) becomes energy-dependent. We then have

$$\gamma_N = \frac{Nq^2\hat{\Gamma}^2(e_{\mathrm{cm}})R(\omega_z)}{m}. \tag{11}$$

This result is equivalent to Eq. (4) but uses the energy-dependent value $\hat{\Gamma}^2(e_{\mathrm{cm}})$ instead of $1/D^2$. Since $\hat{\Gamma}$ increases for smaller e_{cm}, the cooling rate can increase significantly during the cooling process. This can be seen in Fig. 4 for the single-particle case, together with the result of a direct simulation of resistive cooling for a single trapped particle. The rate γ_N behaves correspondingly.

D. Resonator impedance and signal

In the steady state, the voltage at either electrode of the resonator is determined by the complex-valued impedance Z. For a

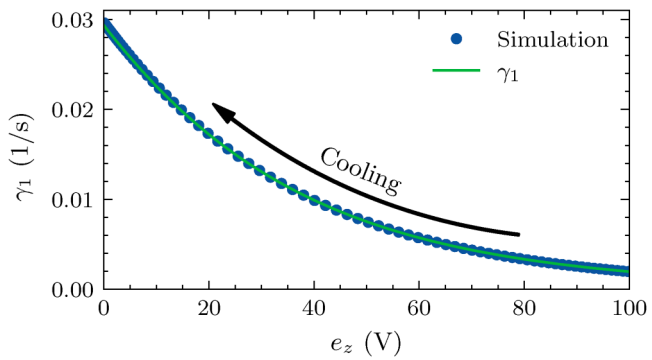

FIG. 4. Energy-dependent single-particle cooling rate for a single trapped Ne^{8+} ion according to Eq. (11), together with the simulation of the cooling process. During the cooling process, the energy e_z decreases. The result was calculated for a resonator with $R = 110\,\mathrm{k\Omega}$.

harmonic driving current I_{ind} with frequency ω_z, the voltage at either electrode is given by

$$U_{\pm} = Z(\omega) I_{ind}. \tag{12}$$

The impedance of the double-pick-up design can be calculated from

$$Z(\omega) = \frac{1}{4} \frac{R_S + iL\omega}{iR_S C_{tot}\omega - \omega^2 L C_{tot} + 1}, \tag{13}$$

and the real part of the impedance is given by $R(\omega) = \Re(Z(\omega))$. The total capacitance $C_{tot} = 22.4(7)\,pF$, inductance $L = 590(20)\,\mu H$, and series resistance $R_S = 449(3)\,\Omega$ of the resonator have been determined independently. At its resonance frequency, the cooling circuit's impedance Z is purely Ohmic and takes the value $Z = R = 2\pi Q L f_R$, where $Q = 11.5$ is the quality factor.[19,20] At the resonance frequency of $f_R \approx 1.38\,MHz$, the value is $Z = R = 14\,k\Omega$. The qualitative behavior of this impedance has been discussed previously.[10,17] A quantitative calculation of the circuit results in the additional factor of $\frac{1}{4}$ seen in Eq. (13). Compared to single-electrode resonators, this factor reduces the signal amplitude U and the cooling rate γ by a factor of four. However, this is compensated by the fact that the amount of current I_{ind} is twice as large since two pick-up electrodes are employed. This results in a smaller signal $U \propto I_{ind}$, but for the resistive cooling $\gamma \propto I_{ind}^2$, both designs result in the same cooling rate.

The quality factor of $Q = 11.5$ is well-suited for the present center-of-mass cooling, since the rate γ_N is still high (of the order of $100\,s^{-1}$) and the large bandwidth of the resonator of $f_R/Q = 120\,kHz$ allows the simultaneous cooling of the entire ion ensemble even in the presence of spurious energy-dependent frequency shifts during cooling.

The principal advantage of the double-electrode configuration (aside from its advantageous off-resonance behavior[17]) is the cancelation of any external electrical noise or disruption, which equally affects both detection electrodes and, thus, does not contribute to the total induced current. This allows the measurements to commence immediately upon capture, since the unavoidable pulse from the fast switch of the trap electrode for dynamic capture does not influence the measurement.

IV. MODEL OF RESISTIVE COOLING

A. Quantities and rate equation

A comparatively simple model can be used to describe the process of resistive cooling in a Penning trap for large particle ensembles under the given conditions. This model has been used to explain experimentally observed cooling behavior of large, pure ion ensembles earlier.[5,9,10,17] The model uses the axial center-of-mass energy e_{cm}, the uncorrelated relative axial energy e_{ax}, and the radial energy e_r which will be ignored in the present application of the model. All energies are expressed in terms of energy per charge and particle. In the model, the energy e_{cm} is cooled at the center-of-mass cooling rate γ_N as given by Eq. (11); in addition, there is an effective energy exchange between e_{cm} and e_{ax} resulting from a change in the relative phases of the axial motions due to the frequency distribution $\Delta\omega_z$ of the trapped particles. This exchange occurs at a rate of γ_{ax}. The model gives a rate equation for e_{cm} that reads

$$\dot{e}_{cm} = -\gamma_N e_{cm} + \gamma_{ax}\left(\frac{e_{ax}}{N-1} - e_{cm}\right). \tag{14}$$

B. Assumptions and validity

This equation assumes that energy e_r from the radial motions does not contribute to the process. This is justified since for the present conditions, the axial-radial coupling due to long-range Coulomb interaction is ineffective and its time scale has been estimated to be $\tau_S \approx 500\,ms$.[10] Hence, in the current experiment, this energy exchange is not observed and can be neglected.

The overall model assumes the energies and frequencies of the center-of-mass and of individual-ion motions relative to it to be well-defined quantities that allow for a statistical treatment. This is true for sufficiently large ensembles of particles ($N \gg 1$), as has been shown previously.[1,9] For the present ion numbers in the range of several tens of thousands, we assume to fulfill this condition. We also assume that the rate of c.m.-cooling is, indeed, given by $\gamma_N = N\gamma_1$, which is justified theoretically as discussed above, and in addition has been experimentally shown over a wide range of ion numbers.[10]

For the application of the presented cooling model to measured curves of induced power P as a function of time, we further assume that the cooling circuit's impedance Z is essentially constant over the center-of-mass frequency range, which is justified at the present resonator bandwidth. As will be shown below, the center-of-mass frequency range in each individual measurement is even smaller than the bandwidth $\Delta f = 510\,Hz$ of the spectrum analyzer used for the signal power measurement, which itself is much smaller than the bandwidth of the resonator of $f_R/Q = 120\,kHz$.

C. Initial cooling and quasi-equilibrium

The expected time evolution of the involved energies e_{cm} and e_{ax} is given by the rate equation (14). It features two rates: the rate of cooling of the axial center-of-mass γ_N and the rate γ_{ax} of axial energy "re-shuffling" between the center-of-mass motion and the relative axial motions ("de-phasing rate"). During the overall cooling process, the value of the axial de-phasing rate γ_{ax} in Eq. (14) is not constant, since it is given by the width of the axial frequency distribution $\Delta\omega_z$[1] that typically changes during storage on account of various effects.[9] For the present conditions (injection of a well-defined bunch), it is of the order of $10\,s^{-1}$ directly upon capture[10,17] such that the center-of-mass cooling of the coherently moving ions is the dominant process initially. It leads to an initial decay of e_{cm} at the rate $\gamma_N = N\gamma_1$ [Eq. (4)], which continues until a quasi-equilibrium is reached between the center-of-mass cooling and energy re-shuffling due to axial de-phasing. In this quasi-equilibrium, Eq. (14) and the condition $\dot{e}_{cm} = 0$ result in

$$\bar{e}_{cm} = \frac{\bar{\gamma}_{ax}}{\gamma_N + \bar{\gamma}_{ax}} \frac{\bar{e}_{ax}}{N-1}, \tag{15}$$

where the bar indicates the respective quasi-equilibrium values. Presently, the quasi-equilibrium value $\bar{\gamma}_{ax}$ is expected to be

significantly larger than the initial value of γ_{ax} because of the expected increase of the axial frequency width during storage.[9,17] Once this quasi-equilibrium is reached, the particle ensemble has lost its initial phase coherence and cooling of the total energy is limited to the single-particle cooling rate. The energy flow into the cooling circuit is limited, since in equilibrium, the center-of-mass energy is $1/N$ of the total axial energy $\bar{e}_{ax}$, as expected and observed for ion ensembles with random phase distributions.[1,3,9] This limitation is due to the comparatively small signal induced in the cooling circuit by an incoherently moving particle ensemble. This is independent of the energy and rate of conversion from incoherent axial motion into the center-of-mass motion; hence, large values of $\bar{e}_{ax}$ and $\bar{\gamma}_{ax}$ do not increase the observed cooling rate in quasi-equilibrium.

D. Fit quantities

Under the same assumptions, once a quasi-equilibrium is reached, the values for $\bar{e}_{ax}$ and $\bar{\gamma}_{ax}$ are essentially constant and the heating of $\bar{e}_{cm}$ by $\bar{e}_{ax}$ can, thus, be described by a constant value of

$$C \equiv \gamma_{ax}\left(\frac{\bar{e}_{ax}}{N-1} - \bar{e}_{cm}\right) = \frac{\gamma_N \bar{\gamma}_{ax}}{\gamma_N + \bar{\gamma}_{ax}} \frac{\bar{e}_{ax}}{N-1}. \tag{16}$$

Inserting γ_N from Eq. (11) into Eq. (14) results in

$$\dot{e}_{cm} = -BR(\omega_z)\hat{\Gamma}^2(e_{cm})e_{cm} + C, \quad B \equiv \frac{q^2 N}{m}, \tag{17}$$

which is used to model the measured energy evolution of captured ion bunches. Finally, the relation between observed power $P \propto U_+^2$ and center-of-mass ion energy e_{cm} is established by inserting Eq. (9) into Eq. (12) to give

$$P = A|Z(\omega_z)|^2\hat{\Gamma}^2(e_{cm})e_{cm}, \quad A \equiv \kappa\frac{q^3}{m}N^2. \tag{18}$$

Here, κ is a dimensionless constant of proportionality that only depends on the amplification and the spectrum analyzer settings. These three equations introduce three parameters: A, B, and C, which characterize the situation. From a fit to a measured cooling curve (observed power P as a function of time), the parameters A, B, and C and the initial center-of-mass energy e^0_{cm} can be obtained. From these, we can in addition calculate the rate of center-of-mass cooling, the energy in the final quasi-equilibrium, and the absolute ion number.

V. MEASUREMENTS AND RESULTS

Bunches of Ne^{8+} were dynamically captured in the Penning trap as described. In order to track the behavior during the resistive cooling process, snapshot spectra of the ensemble were taken for different delays after the initial capture. A selection of these spectra is shown in Fig. 5 to illustrate the general effect of cooling. They show a decay of P by several orders of magnitude within less than 50 ms and a relative shift of the central frequency by about half a percent. The former results from the rapid cooling of e_{cm}, and the latter follows from the residual energy-dependence of the axial

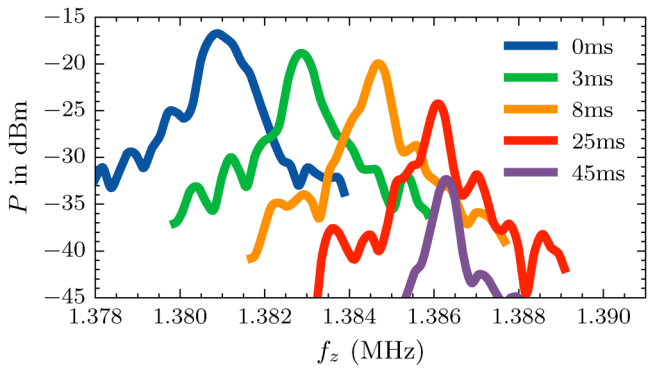

FIG. 5. Selection of snapshot spectra (power as a function of frequency) recorded for different time delays after capture.

frequency in a non-ideal Penning trap. A Gaussian peak model was applied to each of these spectra to determine the peak power P and the central frequency f_z. This is appropriate as the peak shape is determined by the bandwidth of the spectrum analyzer of $\Delta f = 510$ Hz. The fact that the width of each of these peaks is determined by the bandwidth of the spectrum analyzer illustrates that a frequency window of 510 Hz is enough to cover the frequency distribution of the center-of-mass mode in each individual measurement. The shifts of the central frequency result from the resistive cooling of the center-of-mass energy and the resulting motion frequency shifts in a real Penning trap.

The measured time evolution of the peak power P is shown in Fig. 6. For each time, the peak power was determined by a Gaussian fit to a measured spectrum. The resulting curve of measured power P as a function of time shows three main features:

- Initially, in the present case within the first 20 ms, the slope of the curve increases until it becomes essentially constant. This is

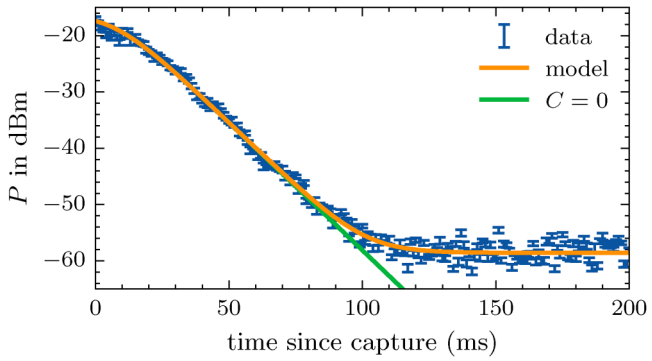

FIG. 6. Measured power P as a function of time after capture. Each point corresponds to a snapshot spectrum as shown in Fig. 5. The orange curve is a fit to the data according to the model, yielding the parameters A, B, and C together with the initial c.m. energy e^0_{cm}. A measurement without any captured ions yields a noise-floor power level of less than −80 dBm.[10]

TABLE I. Parameters of the model fitted to the data shown in Fig. 6. The errors of the fit parameters are 2σ confidence intervals.

Parameter	Value
e^0_{cm}(V)	17.2(4)
A (fA m^2 kΩ^{-2})	1170(90)
B (mm^2 s^{-1} kΩ^{-1})	1030(20)
C (mV s^{-1})	81(6)

due to the initially large amplitudes and, thus, smaller value of the pick-up $\hat{\Gamma}$ and slower cooling [see Eqs. (8) and (9)].
- After that, the curve shows an exponential decay with an essentially constant rate of currently 103(3) s^{-1}, which is in agreement with the expected resistive center-of-mass cooling rate from Eq. (11) for $N = 20\,000$ ions. This ion number is in agreement with the fit result and an independent measurement, as will be discussed below.
- Finally, at present after about 100 ms, the signal reaches the expected quasi-equilibrium where c.m.-cooling occurs at a much smaller rate limited by axial re-shuffling. The model for $C = 0$ (without a quasi-equilibrium state, green curve) fails to describe the data.

Overall, the fit according to the model as expressed by Eqs. (16) to (18) describes the data well (see the orange curve in Fig. 6). In particular, for a value of $C = 0$ the model describes the initial decay but fails to reach equilibrium (green curve in Fig. 6), supporting the assumption that C is only responsible for the equilibrium level reached. The parameters A, B, and C and the initial center-of-mass energy e^0_{cm} have been fitted using lmfit[26] and the result is shown in Table I. As we have used the initial center-of-mass energy as a fitting parameter, it was necessary to solve the equations of motion using a fourth-order Runge–Kutta algorithm.[27]

We can now use the obtained values for the fit parameters to calculate the quantities that characterize the ion bunch and its cooling. Parameter A determines the absolute scale of the measurement by establishing a relation between absolute ion energy and measured power [yielding $\kappa = 42(4)\,\Omega^{-1}$ in Eq. (18)], B determines the center-of-mass cooling rate, C determines the quasi-equilibrium energy, and e^0_{cm} is the initial center-of-mass energy.

A. Initial ion energy

The value of the initial axial ion energy directly upon capture into the trap is a direct result of the fit, so no further calculation is required. In the present example, its value is $e^0_{\mathrm{cm}} = 17.2(4)$ V per charge and ion.

B. Absolute ion number

From fit parameter B, the number of trapped particles N can be determined directly as

$$N = \frac{m}{q^2} B = 20\,800(400). \tag{19}$$

For comparison, 64 measurements of cooling curves were made. From these curves, parameter B was determined and the number of ions is given by

$$N = 21\,000(700), \tag{20}$$

where the error is the standard deviation. For an independent comparison, a calibrated non-destructive image charge detector[14,15] located adjacent to the exit side of the trap was used to measure the absolute number N in the released ion bunch. This yields

$$N = 19\,000(2000), \tag{21}$$

which agrees with the resonator result, demonstrating the ability of the method to determine absolute numbers from recorded cooling curves. The smaller result from the image charge detector may be due to a spurious loss of particles during the release process. As the cooling curve can be measured for each captured ion bunch,[10] the number of ions can be recorded for each individual-ion ensemble directly inside the trap and directly prior to a subsequent measurement.

C. Center-of-mass cooling rate

The expected center-of-mass cooling rate (before reaching the quasi-equilibrium state) is given by Eq. (11). This equation captures the observed behavior of initially slower cooling due to high axial amplitudes and correspondingly less efficient cooling (currently before about 20 ms). After that, the observed rate is essentially constant and can be calculated from the fit parameter B as

$$\gamma_N = BR(\omega_z)\hat{\Gamma}^2(e_{\mathrm{cm}} = 0) = 103(3)\,\mathrm{s}^{-1}. \tag{22}$$

The determined value of γ_N is in good agreement with the result expected from Eq. (11) for the measured ion number from Sec. V B.

D. Equilibrium energy

In equilibrium, the power $\bar{P}$ is determined by the parameter C given by Eq. (16), which depends on the rates γ_N and $\bar{\gamma}_{\mathrm{ax}}$. We assume $\bar{\gamma}_{\mathrm{ax}} \gg \gamma_N$ as will be justified below. Since C is governed by the smaller of the two rates, it can be determined from the measured value of γ_N, which allows the direct calculation of $\bar{e}_{\mathrm{ax}}$

$$\bar{e}_{\mathrm{ax}} = \frac{C(N-1)}{\gamma_N} = 16(2)\,\mathrm{V}. \tag{23}$$

To justify the assumption of $\bar{\gamma}_{\mathrm{ax}} \gg \gamma_N$, we look at the expected width of the axial frequency distribution at that energy in thermal equilibrium,[9]

$$\bar{\gamma}_{\mathrm{ax}} = \Delta\omega_z \approx \frac{3C_4}{C_2}\frac{q\bar{e}_{\mathrm{ax}}}{m\omega_z d^2}, \tag{24}$$

where C_4/C_2 is a measure of the deviation of the actual trap potential from $V \propto z^2$. For the present value of $C_4/C_2 = 0.005$ and the obtained energy $\bar{e}_{\mathrm{ax}}$, $\bar{\gamma}_{\mathrm{ax}} \approx 10\,000\,\mathrm{s}^{-1}$, this justifies the assumption of $\bar{\gamma}_{\mathrm{ax}} \gg \gamma_N$. The result shows that in equilibrium, there is a substantial amount of energy in the uncorrelated mode compared to the

initial center-of-mass energy. Given the initial energy e_{cm}^{0} of 17.2 (4) eV, these two energies combined are in good agreement with the estimated total energy of 30 V per ion and charge. In equilibrium, the center-of-mass energy is negligible ($\bar{e}_{cm} \ll \bar{e}_{ax}$) and the mean energy per charge and particle is, hence, determined by $\bar{e}_{ax}$.

Of the initial total energy per charge and ion, given by the sum of c.m. energy and uncorrelated energy, the center-of-mass component is rapidly cooled to effectively zero, leaving the axial energy in the individual (uncorrelated) motions given by Eq. (23). Hence, the amount of energy that can be cooled away efficiently is determined by the initial relation between e_{cm} and e_{ax}, which can be determined by this method. This is a pre-requisite for an optimization of the ion production, deceleration, and capture process to the end of achieving a high initial degree of energy in the axial c.m. motion ($e_{cm} \gg e_{ax}$), which can be cooled efficiently.

VI. SUMMARY AND CONCLUSION

We have shown that it is possible to determine important properties of captured ion bunches and their resistive cooling behavior from a measured cooling curve of detected power as a function time directly upon capture in a Penning trap. Such a measurement allows for an absolute determination of the initial energy and number of ions in a captured bunch, as well as of the rate of cooling of its center-of-mass motion and of the final ion energy. One pre-requisite for this is the ability to make such measurements immediately after dynamic capture, which is possible due to a dual-electrode resonator design.

The recorded cooling curves have been analyzed with a simple model that allows the direct determination of the mentioned quantities in the given situation. The resulting ion number was independently confirmed by a non-destructive detector, which validates the model of the cooling process and also shows the correct calibration of the dual-electrode resonator.

Once the absolute scale of the measured signal, as expressed by the parameter κ, has been calibrated by the presented method, the characteristic quantities of the bunches can be determined on a shot-by-shot basis. This enables the optimization of the ion-capture process towards low initial energy in the uncorrelated motion, while the center-of-mass energy can be cooled within a few tens of milliseconds. The present detector and methods may quite readily be implemented in a range of Penning trap experiments that work with externally produced particle bunches, as it affords no large deviation from the common schemes for non-destructive detection and cooling.

AUTHOR DECLARATIONS

Conflict of Interest

The authors have no conflicts to disclose.

Author Contributions

Markus Kiffer: Formal analysis (lead); Investigation (equal); Visualization (lead); Writing – original draft (lead); Writing – review & editing (equal). **Stefan Ringleb:** Conceptualization (equal); Formal analysis (equal); Investigation (equal); Visualization (supporting); Writing – original draft (supporting); Writing – review & editing (equal). **Thomas Stöhlker:** Conceptualization (supporting); Funding acquisition (lead); Project administration (lead); Supervision (lead); Writing – review & editing (equal). **Manuel Vogel:** Conceptualization (equal); Project administration (supporting); Supervision (supporting); Visualization (supporting); Writing – original draft (supporting); Writing – review & editing (equal).

DATA AVAILABILITY

The data that support the findings of this study are available from the corresponding author upon reasonable request.

REFERENCES

[1]D. J. Wineland and H. G. Dehmelt, J. Appl. Phys. **46**, 919 (1975).
[2]L. S. Brown and G. Gabrielse, Rev. Mod. Phys. **58**, 233 (1986).
[3]W. M. Itano, J. C. Bergquist, J. J. Bollinger, and D. J. Wineland, Phys. Scr. **T59**, 106 (1995).
[4]M. S. Ebrahimi, Z. Guo, M. Vogel, M. Wiesel, G. Birkl, and W. Quint, Phys. Rev. A **98**, 023423 (2018).
[5]M. Vogel, H. Häffner, K. Hermanspahn, S. Stahl, J. Steinmann, and W. Quint, Phys. Rev. A **90**, 043412 (2014).
[6]W. Shockley, J. Appl. Phys. **9**, 635 (1938).
[7]S. Ramo, Proc. IRE **27**, 584 (1939).
[8]D. F. A. Winters, M. Vogel, D. Segal, and R. C. Thompson, J. Phys. B **39**, 3131 (2006).
[9]M. Vogel, *Particle Confinement in Penning Traps*, 2nd ed. (Springer, 2024).
[10]M. Kiffer, S. Ringleb, Th. Stöhlker, and M. Vogel, Phys. Rev. A **109**, 033102 (2024).
[11]S. Djekic, J. Alonso, H.-J. Kluge, W. Quint, S. Stahl, T. Valenzuela, J. Verdu, M. Vogel, and G. Werth, Eur. Phys. J. D **31**, 451 (2004).
[12]H. Schnatz, G. Bollen, P. Dabkiewicz, F. Kern, H. Kalinowsky, L. Schweikhard, H. Stolzenberg, and H.-J. Kluge, Nucl. Inst. Methods Phys., Sect. A **251**, 17 (1986).
[13]S. Ringleb, N. Stallkamp, M. Kiffer, S. Kumar, J. Hofbrucker, B. Arndt, M. Vogel, W. Quint, Th. Stöhlker, and G. G. Paulus, Phys. Scr. **97**, 084002 (2022).
[14]M. Kiffer, S. Ringleb, N. Stallkamp, Béla Arndt, I. Blinov, S. Kumar, S. Stahl, Th. Stöhlker, and M. Vogel, Rev. Sci. Instrum. **90**, 113301 (2019).
[15]S. Ringleb, M. Kiffer, J. K. C. Ballentin, Th. Stöhlker, and M. Vogel, Sci. Rep. **13**, 22669 (2023).
[16]G. Gabrielse, L. Haarsma, and S. L. Rolston, Int. J. Mass Spectrom. Ion Processes **88**, 319 (1989).
[17]S. Ringleb, M. Kiffer, Th. Stöhlker, and M. Vogel, Eur. Phys. J. Plus **139**, 401 (2024).
[18]G. Maero, F. Herfurth, H. J. Kluge, S. Schwarz, and G. Zwicknagel, Appl. Phys. B **107**, 1087 (2012).
[19]S. Ulmer, H. Kracke, K. Blaum, S. Kreim, A. Mooser, W. Quint, C. C. Rodegheri, and J. Walz, Rev. Sci. Instrum. **80**, 123302 (2009).
[20]P. Horowitz and W. Hill, *The Art of Electronics*, 3rd ed. (Cambridge University Press, 2015).
[21]G. Zschornack, M. Kreller, V. P. Ovsyannikov, F. Grossman, U. Kentsch, M. Schmidt, F. Ullmann, and R. Heller, Rev. Sci. Instrum. **79**, 02A703 (2008).
[22]E. Plies, K. Marianowski, and T. Ohnweiler, Nucl. Instrum. Methods Phys. Res., Sect. A **645**, 7 (2011).
[23]P. Mandal, G. Sikler, and M. Mukherjee, J. Instrum. **6**, P02004 (2011).
[24]S. Coeck, B. Delauré, M. Herbane, M. Beck, V. V. Golovko, S. Kopecky, V. Yu. Kozlov, I. S. Kraev, A. Lindroth, T. Phalet, D. Beck, P. Delahaye, A. Herlert, F. Wenander, and N. Severijns, Nucl. Instrum. Methods Phys. Res., Sect. A **572**, 585 (2007).
[25]S. Brewer, N. Guise, and J. Tan, Phys. Rev. A **88**, 063403 (2013).
[26]M. Newville, "LMFIT: Non-linear least-square minimization and curve-fitting for python" Zenodo (2014).
[27]J. Dormand and P. J. Prince, J. Comput. Appl. Math. **6**, 19 (1980).